Energy Reports 7 (2021) 5431–5445

Contents lists available at ScienceDirect

Energy Reports

journal homepage: www.elsevier.com/locate/egyr

Research paper

Prediction of the effects of climate change on hydroelectric generation, electricity demand, and emissions of greenhouse gases under climatic scenarios and optimized ANN model

Li-Na Guo [a,1], Chen She [b,1], De-Bin Kong [a], Shuai-Ling Yan [c,*], Yi-Peng Xu [d,1], Majid Khayatnezhad [e], Fatemeh Gholinia [f]

[a] Department of Mathematics and Physics, Yantai Nanshan University, Yantai 265700, China
[b] School of Economics and Management, Tiangong University, Tianjin, 300387, China
[c] Department of Mathematics and Computer Science, Hengshui University, Hengshui 053000, Hebei, China
[d] School of Mathematical Sciences, Tiangong University, Tianjin 300387, China
[e] Department of Environmental Sciences and Engineering, Ardabil Branch, Islamic Azad University, Ardabil, Iran
[f] Department of Watershed Management, University of Mohaghegh Ardabili, Ardabil, Ardabil Province, Iran

ARTICLE INFO

Article history:
Received 2 April 2021
Received in revised form 26 July 2021
Accepted 19 August 2021
Available online 6 September 2021

Keywords:
The climatic parameters
Artificial neural network
The improved electromagnetic field optimization (IEFO) algorithms
Hydropower generation
The greenhouse gas emission

ABSTRACT

In this study, an attempt is made to manage the gap between energy demand and energy supply by predicting hydropower production, energy demand, and greenhouse gas emissions. The interaction between climatic, hydrological, and socio-economic parameters creates a nonlinear and uncertain relationship. The complexity of this nonlinear relationship necessitate the use of ANN to estimate energy demand. To predict energy demand, ANN model is used along with improved Electromagnetic Field Optimization (IEFO) algorithms. The results show, hydroelectric generation in the near future under RCP2.6, RCP4.5, and RCP8.5 is decreased 10.981 MW, 12.933MW, and 14.765MW and in the far future decreased 21.922 MW, 23.649 MW, and 26.742 MW. The energy demand increases in the near future 513 MW and far future 1168 MW. According to forecasting hydropower generation and energy demand, the gap between the demand-supply will increase. Also, the greenhouse gases emissions is increase due to the increase in fossil fuel consumption.

1. Introduction

Climate change due to global warming is the result of increasing greenhouse gas concentrations, which is the most important environmental problem of the present age on a global scale. Climate change is a phenomenon that occurs on a long-term scale and several thousand years (Ghiasi et al., 2019). Recently, with the development of industry and population growth, the trend of climate change has accelerated. Climate change has caused environmental problems, such as changes in precipitation patterns, the melting of polar glaciers, and rising sea levels (Huangpeng et al., 2021). The main cause of these changes is global warming (Mir et al., 2020). Rising global temperatures are the result of rising greenhouse gases and excessive absorption of energy from the Earth's atmosphere. Rising greenhouse gases have disrupted the energy balance between the solar and the Earth (Ren et al., 2021).

In recent decades, with apparent evidence of climate change, concern about the planning and operation of water resources has increased (Xu et al., 2020). Changing the amount of incoming runoff to the reservoirs of hydroelectric dams is one of these undesirable consequences. According to global reports, about 16% of the world's electricity and 70% of the world's renewable electricity is generated from hydropower (Feng et al., 2018). The many benefits of hydropower generation, including its very low cost and lack of greenhouse gas emissions, make it one of the most popular sources of energy production worldwide. Therefore, it is necessary to assess the vulnerability of hydropower systems in the face of the consequences of climate change (Jakimavičius et al., 2020).

Today, due to the increasing costs of fossil fuels to provide the energy needed by human societies, hydropower projects have a very high economic justification. In this regard, the construction of hydropower plants as a low-cost resource has been considered by most countries in the world (Xu et al., 2020). China also has good conditions for the construction and operation of hydropower plants (Meng et al., 2020). Hydropower plants are considered as the most important parts of transmission and distribution networks as power generation sources (Wang et al.).

* Corresponding author.
E-mail address: yanshuailing@163.com (S.-L. Yan).
[1] These authors contribute equally to this paper.

https://doi.org/10.1016/j.egyr.2021.08.134

Energy is essential for economic development, agriculture, and industry (Cai et al., 2019). Energy plays a significant role in economic prosperity, social welfare, and industry development (Li et al., 2021). Due to population growth, increasing per capita electricity consumption, development of industrial sectors, the energy demand is increasing (Yu and Ghadimi, 2019). Lack of energy in meeting the needs of economic activities leads to stagnation or reduction of economic growth as well as lowering living standards (Liu et al., 2017). The dependence of lifestyle on energy has made it impossible to imagine life without equipment and machinery (Antonopoulos et al., 2020). Energy demand analysis is one of the most important issues in developing countries (Chen et al., 2016). Therefore, it is important to use analytical methods to better understand energy demand. To supply the energy needed by consumers, the grid load must be predicted in the coming years and planned for grid development and power supply (McGookin et al., 2021).

The interaction between climatic parameters (temperature and rainfall) and hydrological parameters (inlet runoff to the hydroelectric reservoir) and socio-economic parameters (population and GDP) creates a nonlinear and uncertain relationship (Yuan et al., 2020). The complexity of this nonlinear relationship, the large number of parameters, and the difficulty of measuring these parameters necessitate the use of ANN to estimate energy demand. Experimental models cannot be used to forecast non-linear electricity demand behavior concerning climatic, hydrological, and socio-economic parameters. Therefore, to evaluate this relationship, the use of data-driven models such as ANN is of interest to researchers (Unutmaz et al., 2021).

Many studies have examined how electricity demand, hydropower generation changes under the influence of climatic changes, which can be referred to in the following researches (Yu et al., 2020). Di Piazza et al. (Di Piazza et al., 2021) forecasted manage electrical network using a time series neural network-based model. In this study, the Artificial Neural Network (ANN) was used to predict short-term hourly electricity demand. The results showed that the ANN model was more suitable for short-term prediction compared to linear regression methods (Ye et al., 2020). Simulation analysis by the ANN model showed the advantage of the proposed method. This model can predict short-term electricity demand with a very simple network structure and at the lowest cost.

UNUTMAZ et al. (Unutmaz et al., 2021) projected energy demand applying Artificial Neural Networks (ANNs) model. Socio-economic, technological, and demographic parameters were used to increase the accuracy of energy forecasting. The results of the forecasts show that the electricity demand for the next 15 years will have the best estimate and provide accurate results using the proposed method.

Khalil et al. (2019) investigated energy efficiency using artificial neural networks. The results showed that after training and validation of the artificial neural networks, it has the best forecast for energy efficiency. So that the accuracy of validation of this model is 60.99% that provided acceptable results.

Mason et al. (2018) Projected electricity demand and carbon dioxide emissions in Ireland by evolutionary neural networks model. In this research, covariance matrix adaptation evolutionary strategy metaheuristic algorithm was used to train the neural network to simulate the neural network prediction more accurately. The results of the trained neural network showed that this model provides fast convergence, strong performance, and a more accurate prediction of energy demand and carbon dioxide intensity.

Franco and Sanstad (2008) examined climate change and energy demand in California. The results of predicting the impact of climate change on California's energy demand show that possible temperature changes will have a significant impact on electricity consumption and increased demand. It also changes the economic cost of electricity.

Emodi et al. (2018) examined the short- and long-term effects of climate change on Australian electricity demand. In this study, four scenarios based on Representative Concentration Pathways (RCP) were used to predict climate change. The results showed that electricity consumption will have a gradual increase due to rising temperatures in winter. The results of forecasts showed that the peak of electricity consumption will be in summer.

Tan and others (2021) the impact of climate change on power fluctuations in China. Climate change directly affects electricity demand and can disrupt the operation of the electricity grid. In this study, they used an econometric model to analyze the effect of high and low temperatures on energy demand. The results show that high temperature has a positive effect on residential electricity demand while low temperature has a negative effect.

Chen et al. Predicted monthly snowfall due to climate change in Tianjin, China. The forecast results showed that climate change has severe effects on the frequency and intensity of peak monthly electricity demand. In particular, in 2099 under the RCP8.5 scenario, electricity demand in July will be 56% higher than in November. Climate change may cause major changes in the power supply chain.

Garrido-Perez et al. (2021) examined the impact of climate change on Spain's electricity demand. In this study, the RCP8.5 scenario was used to predict climate change. The results show that in the middle of the century, in summer, especially in June and September, 50% of the days will be in strong demand for electricity. And by the end of the century, 90% of the day there will be strong electricity demand. Of course, the electricity demand varies in different parts of the country.

Previous research has shown that the proposed method to predict energy demand is the Artificial Neural Networks (ANNs) (Razmjooy and Estrela, 2019). The results of previous research showed that the ANN method has better results compared to simpler methods such as linear regression. In the mentioned researches, optimization methods have not been used to evaluate the effect of climate change on hydropower generation and energy demand (Hu and Navid, 2020). However, in some studies, optimization methods have been used to develop the artificial neural network to achieve more accurate results (Liu et al., 2020). Although optimization gives a more acceptable prediction, the optimization itself has shortcomings that can affect the predicted results. Optimization methods are sometimes trapped in local optimization. Also, early convergence, rapid speed, and the trade-off between exploration and exploitation are other shortcomings of optimization (Fatemi and others, 2019). These weaknesses decrease the accuracy of the predicted results, so these shortcomings should be addressed by achieving more accurate results. Accurate knowledge of future energy demand can help manage the supply and demand of energy generated by the hydropower plant (Fan et al., 2020). In this study, the energy demand of a new case study is investigated, which not only has not been optimized so far but the meta-heuristic algorithm has not been applied (Ramezani et al., 2021). Also, according to the principle No Free Lunch Theorem there is no optimization algorithm that can solve all optimization problems. Beside the metaheuristic algorithm the advantages, they have disadvantages that can be changed according to different methods (Navid et al., 2021). Therefore, in this research, we have designed an improved method of the Electromagnetic Field Optimization (EFO) algorithms to get the best answer to optimize the energy demand of the Sefidrood dam. In this research, by solving the optimization problems and improving this method, we have tried to predict the electricity demand with maximum accuracy (Guo et al., 2021).

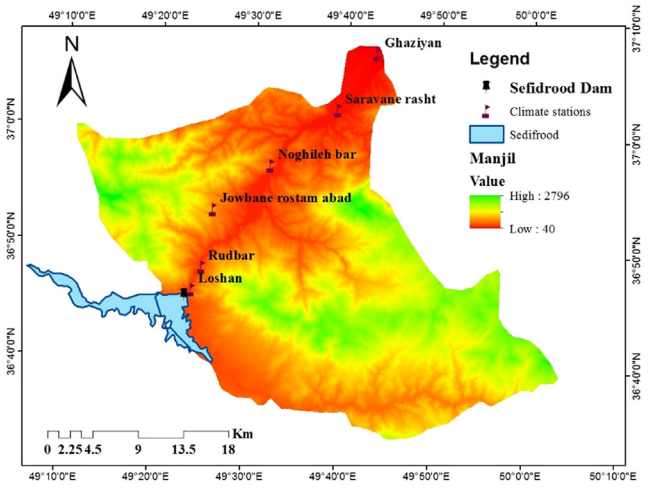

Fig. 1. Manji Dam.

The novelty of this research is the use of the artificial neural network (ANN) optimized by the Improved Electromagnetic Field Optimization (IEFO) algorithms. By improving this algorithm and training the ANN by this improved algorithm will achieve better results (Hosseini et al., 2012). Because based on the proposed method, optimization problems will be solved and the obstacle for more accurate prediction will be removed. This proposed method can also be applied in areas with similar geographical, hydrological, socio-economic characteristics and can be adjusted for other research.

The rest of the paper is organized as follows. Section 1 refers to the introduction that contains the literature review, motivation, and contribution. Section 2 contains the research methodology. Section 3 contains the results and discussion. Section 4 contains the conclusions and policy implications. All the sections have been described in order.

2. Method and material

2.1. Description case study

Manjil watershed has been placed in Gilan province, Iran. Manjil watershed has a high potential to generate power. Sefidrood dam has been located at the beginning of the Sefidrud River. The geographical location of this dam has been located 36° 45′31.27″ N and 49° 23′16.03″ E. Fig. 1 demonstrations the location of the Sefidrud Dam and the geographical location of climate stations.

In this study, the Had-Gem2-Es climate model under Representative Concentration Pathways (RCPs) has simulated temperature, evaporation, and precipitation. The temperature and precipitation parameters have been used to simulate the inlet runoff to the reservoir by the hydrological SWAT model. Then, the Intel runoff has been applied to calculate hydroelectric power generation (Razmjooy et al., 2016). In the other part, using the improved artificial neural network and inputs of climatic parameters simulated by the Had-Gem2-Es climate model under RCPs and socio-economic parameters of energy demand simulated. The socio-economic parameters that are used in this study include Gross Domestic Product (GDP) is the per capita output, population, and electricity price (inflation). The population is collected by the Statistical Center of Iran (SCI, 1965). GDP per capita is gained by statistical data of the Organization for Economic Cooperation and Development (OECD, 1948).

Inflation is given by the global inflation database (Inflation, 0000). The electricity demand dataset has been taken from Gilan Electricity Distribution Company (GEDC, 1947). Hydrological and meteorological data have been obtained by meteorological stations. Finally, the gap between supply–demand under the influence of greenhouse gas concentration is examined with the help of forecasting hydropower generation and energy demand under the influence of changes in climatic parameters. Fig. 2 shows the Methodology framework.

2.2. Climate parameter simulation

Had-Gem2-Es series models are one of the most popular models GCMs are globally certified 3. The horizontal separation is 25.1 degrees latitude and 875.1 degrees longitude. The Had-Gem2-Es model with a spatial resolution of 1.88 × 1.25 km, due to less difference and higher adaptation than the observed data, has a greater ability to predict future loads. Therefore, in this study, the Had-Gem2-Es have been used to simulate climate parameters. To downscale climate, parameters have been utilized the Lars-WG model (Martínez-Solanas and others, 2021). This model converts large-scale climatic variables to regional-scale climatic variables. The Had-Gem2-Es based on the Representative Concentration Pathways (RCPs) scenarios predict climate change (Toste et al., 2018). Fig. 3 shows Representative Concentration Pathways (RCPs) scenarios.

2.3. Hydrological parameter prediction

There are many models to simulate the inflow to the reservoir that can examine the impact of climate change on hydropower generation. In addition to climatic parameters, hydrological phenomena also affect hydropower generation. One of the most important hydrological phenomena is the inlet runoff to the reservoir, which can affect the inlet flow to the turbine and cause changes in power generation by generators. Due to the importance of the inflow to the reservoir and its effect on hydropower generation. In this research, an attempt has been made to simulate the most accurate inlet runoff to the landfill using the best method (Fonseca and Santos, 2019). Distributed hydrological models are of great importance in interpreting and predicting the effect of climate on runoff. In this research, the distribution model of soil and water assessment tool has been used to estimate the runoff entering the dam reservoir. There are many models for hydrological assessment of the basin that are used by water resources managers, decision-makers, and researchers (Faiz et al., 2018). These models are of great help in determining runoff. Continuous flow models can have a better understanding of the hydrological response of the basin Oo et al. (2020). The SWAT model is a distribution-physical model (Bhatta et al., 2019). Which is used to predict the impact of climate on the runoff entering the reservoir of Sefidrud Dam. Meteorological data required in the SWAT model include rainfall, maximum and minimum temperature. In addition to climatic parameters, GIS maps generated in the Arc environment are used to simulate the inlet flow to the reservoir. This information includes a Digital Elevation Map (DEM), soil map, and land-use map.

2.3.1. USDA-NRCS CN method

To simulate runoff the Natural Resources Conservation Service (NRCS) is used. Based on the NRCS method runoff can estimate the following equations (Kassem et al., 2019).

$$R = \frac{(P_r - Ia)^2}{(P_r - Ia) + r} \tag{1}$$

where, P_r shows the entire rainfall (mm), R is the extra rainfall (mm), Ia ($\cong$ 0.25) defines the primary runoff value, and r

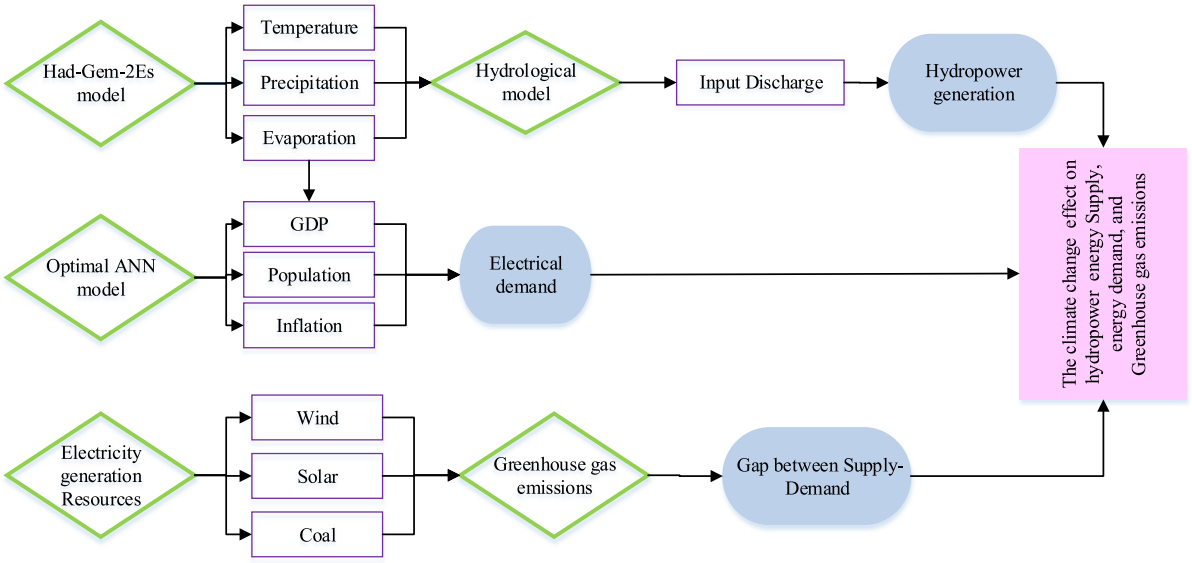

Fig. 2. Flowchart methodology.

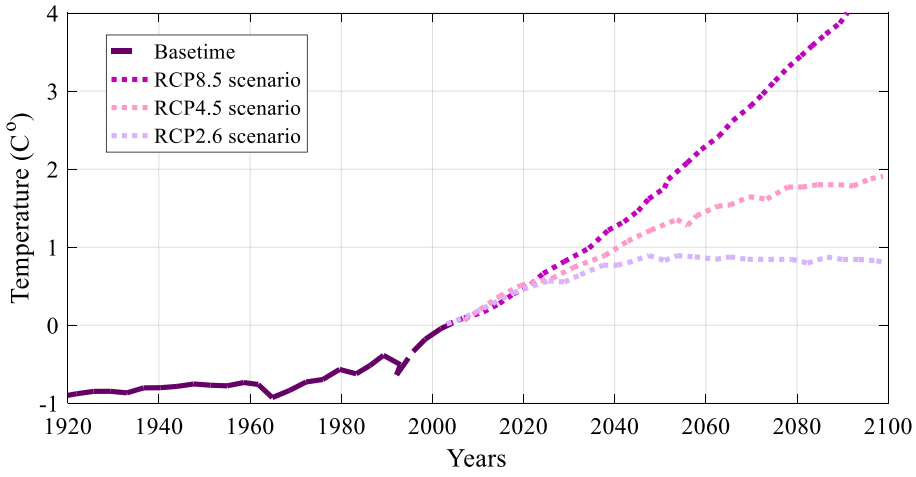

Fig. 3. The Representative Concentration Pathways (RCPs) scenarios.

show the maximum retention value (mm). The retention value is determined by the following equations (Lee et al., 2019).

$$r = \frac{25400}{CN} - 254 \tag{2}$$

where, (CN) defines the Curve Number value which is the initial factor in hydrology to predict runoff from extra rainfall. In natural moisture conditions, the CN value is determined based on watershed characteristics such as soil type, hydrological conditions of the region, land use conditions, and initial soil moisture conditions (Lal et al., 2019).

2.3.2. Improved NRCS-CN for the SWAT model

To estimate the CN value in the SWAT model the r value is used. This value depends on the soil moisture. This value in the SWAT model is calculated by the following equation (Lee et al., 2019).

$$r = r_{max}\left(1 - \frac{SH}{[SH + \exp(x_1 - x_2 RW)]}\right) \tag{3}$$

where, r_{max} is the most retention per day (mm), SH show relative to soil humidity in all profiles except water at the wilting point (mm). The x_1 and x_2 are factor shape coefficients are calculated by the following Equations (Neto et al., 2019).

$$x_1 = \ln\left[\frac{SM}{1 - r_3 S_{max}^{-1}} - SM\right] + w_2 \tag{4}$$

$$x_2 = \frac{\left(\ln\left[\frac{SM}{1-r_3 S_{max}^{-1}} - SM\right] - \ln\left[\frac{Vs}{1-2.54 S_{max}^{-1}} - Vs\right]\right)}{(Vs - SM)} \tag{5}$$

where, SM defines the soil moisture value (mm), S_{max} shows the most retention factor value, r_3 describes the relevant retention factor, and Vs shows the water volume completely saturated.

2.4. Hydropower estimation

Hydropower generation is determined by converting the kinetic energy of water into the energy of electricity. The turbines convert kinetic energy to electricity. Calculate hydropower generation can determine based on the following equation (Dehghani et al., 2019).

$$H_P = \frac{\rho g \times \eta \times \Delta H \times r_t}{10^6 \times n} \tag{6}$$

where ρ is water density (1000 kg/m^3), g is earth's gravity (9.807 m/s^2), ρg defines the water-specific weight, η shows the efficiency of the hydropower station, ΔH is the difference between the upstream and downstream, r_t defines the total input runoff, and n show the evaluation coefficient.

ΔH is determined using the following equation :

$$\Delta H = \left(\frac{H_{up} - H_{down}}{2}\right) - T_r \tag{7}$$

where, ΔH defines the difference between the upstream and downstream that is call water head, H_{up} shows the maximum water levels, H_{down} defines the minimum water level, and T_r defines tailwater.

2.5. Energy demand prediction

The development of industry in societies and the increase in the level of well-being of individuals have increased the energy demand. Therefore, the need to anticipate energy demand is essential for better energy management and supply. Predicting energy demand helps to be aware of the behavior of applicants (Fan et al., 2013). There are several ways to predict energy demand. Like regression and fuzzy methods and neural networks (Kim et al., 2019). Among the methods used to predict energy demand, the artificial neural network method is more efficient. Because the artificial neural network method has a high ability to analyze data and more flexibility than other methods. According to these advantages, in this research, the artificial neural network is used to predict energy demand, which in the next section is the completely artificial neural network (Kitessa et al., 2021).

2.6. Artificial Neural Network (ANN) method

It is simulated based on the behavior of the human nervous system. The artificial neural network, like the neural network of the brain, can receive information and train and process information. This model has three layers of input, middle, and output layers (Yu et al., 2019). Each of these layers in turn has its duty. The input layer receives the parameters needed to predict. The inputs required for the simulation energy demand are socio-economic parameters and Meteorology parameters. Socio-economic data that is used as input data are population, GDP, Inflation. Meteorology parameters are temperature, precipitation, and evaporation. The next section describes the artificial neural network and its improved method. The middle node process input data. Finally, the output node provides the Results of data processing and energy demand prediction (Dinaharan et al., 2020).

The output of each neuron is calculated using two steps. In the first step, the sum of the total weight of input data is obtained, so that the following equation can be used.

$$T_i = \sum_{j=1}^{n} x_{ij} i_i + c_j \tag{8}$$

where, t_i shows the input data number, c_j defines the bias-related weight of the middle node, x_{ij} denotes the input node weight.

In the second stage, the activation function has been applied to provide the output of the ANN model. There are several methods for activation functions. In this research, the sigmoid function has been used that is calculated based on the following equation:

$$Q_j(x) = \frac{1}{1 + e^{-z_j}} \tag{9}$$

Then, the output calculated by the following equation:

$$Out_i = \sum_{j=1}^{n} x_{kj} i_i + c_k \tag{10}$$

Fig. 4 denotes the structure of the ANN model.

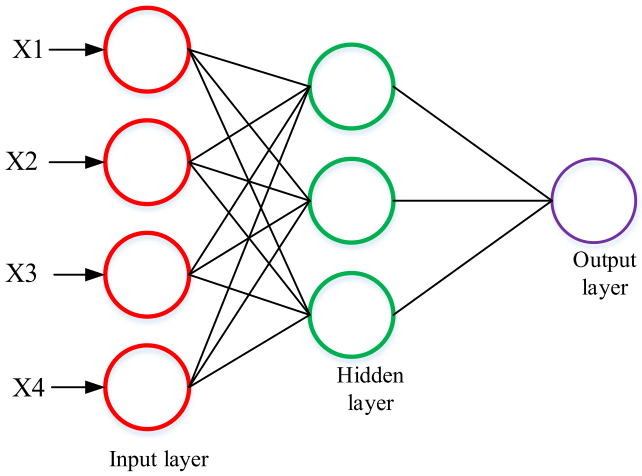

Fig. 4. The structure ANN method.

2.7. Optimization method

2.7.1. Description of electromagnetic field optimization algorithm

There are two types of currents in an electric magnet, one is electric current and the other is magnetic current. Electric magnets have two positive and negative poles, which change based on the direction of the electric current. In addition to electric and magnetic current, there are two types of repulsive and absorption forces in electric magnets. The repulsive force is created when magnets with two similar poles are placed next to each other. Absorption is created when two opposite poles of magnets are placed next to each other. Absorption is about 5%–10% stronger than repulsion (Le et al., 2021). The field Optimization (EFO) algorithm uses theories of the theory of absorption and repulsion to replace the ratio of absorption and forces of absorption with the golden factor. This helps the particles to sufficiently explore the problem area and find the optimal solution (Abedinpourshotorban et al., 2016). EFO is inspired by the behavior of magnetic particles. In this optimization algorithm, every response vector is determined based on a set of electromagnetic particles. The number of electric magnets for electromagnetic particles is determined by the number of parameters of the optimization problem. Therefore, the electromagnets of the electromagnetic particles are optimized based on the problem parameters. Besides, the poles of electromagnetic magnets are the same as those of electromagnetic particles. However, any electromagnetic particle uses the force of absorption or repulsion on the magnet, which is related to the same optimization factor. The Electromagnetic Field Optimization (EFO) algorithm consists of four principal stages: primary population generation, local search, assessment of the all force vector for any individual, going in the path of the input force vector, and managing local neighborhood search to gain the local optimal. The pipeline stages to use the EFO algorithm are described based on the following. In the first step, each individual is randomly made of electromagnetic particles and the cost value of each particle is estimated. It is then assorted into three groups and a segment of the electromagnetic individuals is distributed to the groups. These three groups include the positive field, the negative field, and the neutral field. The positive field contains the most electromagnetic particles and has the highest ratio. The negative field contains particles with a negative polarity that has the lowest ratio. The third group, called neutrals, are zero-negative particles. When particle production, if the produced particle gives acceptable results compared to a poor electromagnetic particle, it is located in a class of the population due to its cost value,

otherwise, it disappears. The algorithm continues until the most iteration is achieved. The coexistence of the two forces of attraction and repulsion of electric magnets and the new response, through distancing themselves from poor solutions and approximating acceptable solutions, cause operational exploration and fast convergence. However, to maintain diversity and avoid local minimums, it must be accidentally stored in the EFO algorithm. Hence, in some particles, there is only one electromagnet that is produced by other electromagnets. The EFO algorithm can be expressed mathematically by the following equation:

$$EMP_j^{New} = EMP_j^{K_j} + \left((\phi \times r) \times \left(EMP_j^{P_j} - EMP_j^{K_j}\right)\right) - \left(r \times \left(EMP_j^{N_j} - EMP_j^{K_j}\right)\right) l \tag{11}$$

where, r shows the accidental value that is between 0 to 1, EMP indicates the electromagnetic particle, j shows a parameter (magnet) index, K is the accidental index of the neutral field, and P is the accidental index of the positive and N shows negative fields produced for the particle's electromagnetic. Eq. (5) is utilized to generate a new particle. Three numbers particles are utilized to make a new particle. Eq. (5) the first part assesses the range between randomly selected particles in the neutral field and the positive field using Eq. (6). Besides, the second part assesses the range between randomly selected particles in the negative field and is a neutral field using Eq. (7). Eq. (6) add as a neutral magnetic random fraction of the estimated range is used. The positive field force is most than the negative force. Therefore, in Eq. (8), the estimated distance between neutral and positive magnets is obtained by multiplication. ϕ (Nearly 1.6) that based on experimental analysis, it is confirmed to have the best performance. Therefore, with integration Eqs. (6)–(8), Eq. (5) is gained.

$$D_j^{P_jK_j} = EMP_j^{P_j} - EMP_j^{K_j} \tag{12}$$

$$D_j^{N_jK_j} = EMP_j^{N_j} - EMP_j^{K_j} \tag{13}$$

$$EMP_j^{New} = EMP_j^{K_j} + \left((\phi \times r) \times D_j^{P_jK_j}\right) - \left(r \times D_j^{N_jK_j}\right) \tag{14}$$

2.7.2. Improved Electromagnetic Field Optimization Algorithm (IEFO)

The literature shows that the electromagnetic field optimization algorithm provides acceptable results to optimize problems, nevertheless, in some time, it has a significant weakness. (Song et al., 2019; Bouchekara et al., 2017; Bouchekara, 2020). As can be seen, when individuals are randomly selected in each production, there is a possibility of early convergence that can reduce the predictive accuracy of energy demand. There are several ways to solve this problem of the optimization algorithm. One of the most successful methods used in this research is the use of the Lévy flight (LF) method (Ingle and Jatoth, 2019). The LF method based on the random behavior to manage local situations is expressed as follows:

$$LF\,(w) \approx \frac{1}{w^{1+\tau}} \tag{15}$$

$$w = \frac{A}{|B|^{\frac{1}{\tau}}} \tag{16}$$

$$\sigma^2 = \left\{\frac{\sin(\pi\tau/2)}{2^{(1+\tau)/2}} \times \frac{\Gamma(1+\tau)}{\tau\Gamma((1+\tau)/2)}\right\}^{\frac{2}{\tau}} \tag{17}$$

where, w shows the step size, $\tau = 1.5$ shows the LF method (Li et al., 2018), $\Gamma(.)$ is the Gamma function, and $A, B \sim N(0, \sigma^2)$. Based on the LF method, the updating formulation is improved based on following equation:

$$EMP_j^{New} = \begin{cases} EMP_j^{K_j} + \left((\phi \times Lf(\sigma) \times r) \times D_j^{P_jK_j}\right) \\ - \left(Lf(\sigma) \times r \times D_j^{N_jK_j}\right), rand > 0.5 \\ EMP_j^{K_j} - \left((\phi \times Lf(\sigma) \times r) \times D_j^{P_jK_j}\right) \\ - \left(Lf(\sigma) \times r \times D_j^{N_jK_j}\right), rand \le 0.5 \end{cases} \tag{18}$$

Also, the Chaos method has been used to improve the algorithm globalization to avoid local optimization. The Chaos method has been achieved by the following equation:

$$C_{i+1}^j = f\left(C_i^j\right), j = 1, 2, \ldots, L \tag{19}$$

where, L is the dimension for the map and $f\left(C_i^j\right)$ is the generator function (Rim et al., 2018).

In this research, the sinusoidal chaotic map is utilized. So, this method refines the local optimization problem, wrong solution, and early convergence. This term has been used to a random value, r, i.e.,

$$r_{k+1}^{new} = a\left(r_k^{new}\right)^2 \sin\left(\pi r_k^{new}\right), \tag{20}$$

where, k is the number of iterations.

Table 1
Features of the studied algorithms.

Metaheuristic Algorithm	Parameters	Value
Ant lion Optimizer (ALO)	w	[2, 6]
	No. search agents	50
Whale Optimization Algorithm (WOA)	$\vec{a}$	2
	$\vec{r}$	1
Locust Swarm Optimization (LS)	F	0.6
	L	1
	g	20

2.7.3. Validation of the suggested algorithm

The value of total algorithms for the population size is 140 and for the iteration, numbers are 200. To give a satisfactory result from the performance of the suggested optimization algorithms has been used the different studied optimization algorithms. These optimization algorithms are Ant lion optimizer (ALO) (Roy et al., 2019) , Whale Optimization Algorithm (WOA) (Mirjalili and Lewis, 2016), Locust Swarm Optimization (LS) (Chen, 2009), the original Electromagnetic Field Optimization (EFO) algorithms (Bouchekara, 2020). Table 1 illustrates the features of the studied algorithms.

Also, Descriptions of each of the studied algorithms and their flowcharts are mentioned in the following subsection:

2.7.3.1. Ant lion Optimizer (ALO). Ant lion optimization algorithm has been suggested by Mirjalili (Leaf-nosed bat, 2009). These algorithms have been inspired by the hunting behavior of ant lions. The principal idea of the ALO algorithm is the food search behavior of Antilles larvae. This optimization algorithm simulates through the interaction between antlions and ants in the trap. To model interactions between antlions and ants, ants must go through the search space, let the ant hunt them, and become more fit through traps. This algorithm involves exploring by random walking and random choice of factors. Exploitation is made by traps. Fig. 5 show the flowchart of Ant lion Optimizer (ALO).

2.7.3.2. Whale Optimization Algorithm (WOA). The Whale Optimization Algorithm (WOA) has been suggested by Mirjalili and Lewis (Mason et al., 2018). This optimization algorithm is inspired

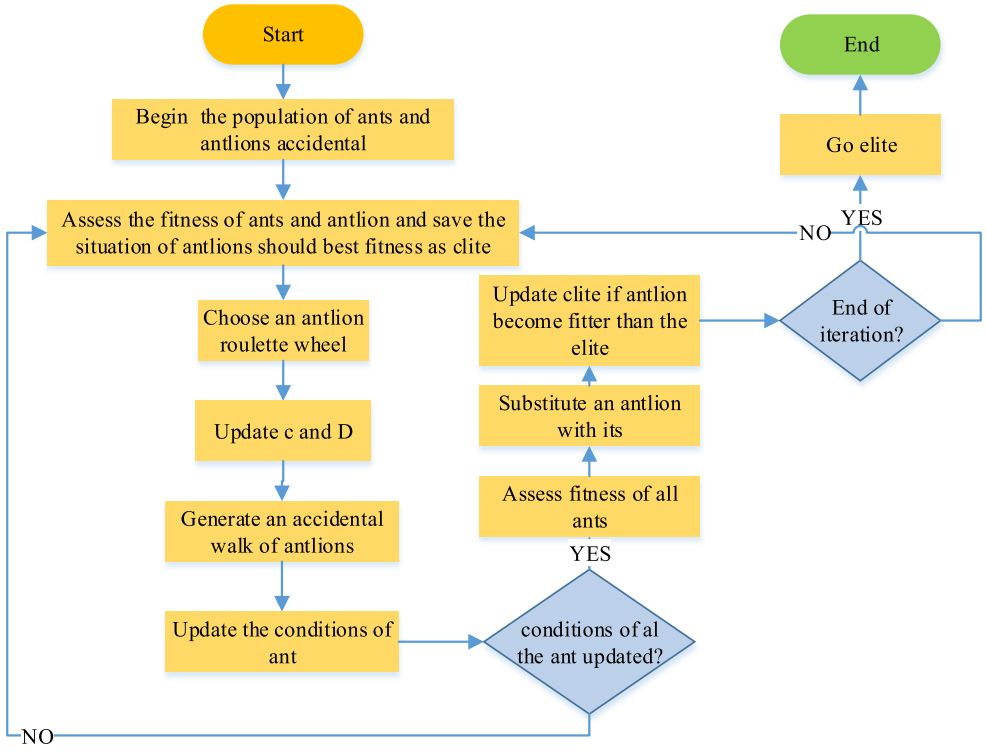

Fig. 5. Ant lion Optimizer (ALO).

by the humpback whale hunting behavior. In this behavior, the whale surrounds the prey by identifying the hunting ground by producing waves. In this algorithm, through imitating the hunting behavior of the humpback whale, the best solution to solve the optimization problem is presented. The assumption of this algorithm in presenting the best candidate solution is the prey of the target or close to optimal. After determining the most suitable search agent, other search agents attempt to update their conditions toward the most suitable search agent. Fig. 6 shows the flowchart of the Whale Optimization Algorithm (WOA).

2.7.3.3. Locust Search Optimization (LS). Locust Search Optimization (LS) has been proposed by Cuevas et al. (2016). *Locust Search (LS) is a global optimization algorithm. It is simulated based on the behavior observed in the category of desert locusts.* In this algorithm, two types of locust behavior have been considered. Individual and social behavior of locusts. In this algorithm, the individual behavior and the society of locusts interact with each other to provide the best solution to find the optimization problem. Fig. 7 show the flowchart of Locust Search Optimization (LS).

Also, the number of the benchmark functions has been used to validate the proposed algorithm efficiency that each of them is described in Table 2.

Fig. 8 shows a two-dimensional version of the benchmark functions for more explanation.

After validating the proposed model, it is used to optimize the artificial neural network to forecast energy demand that the results have been explained in the following section.

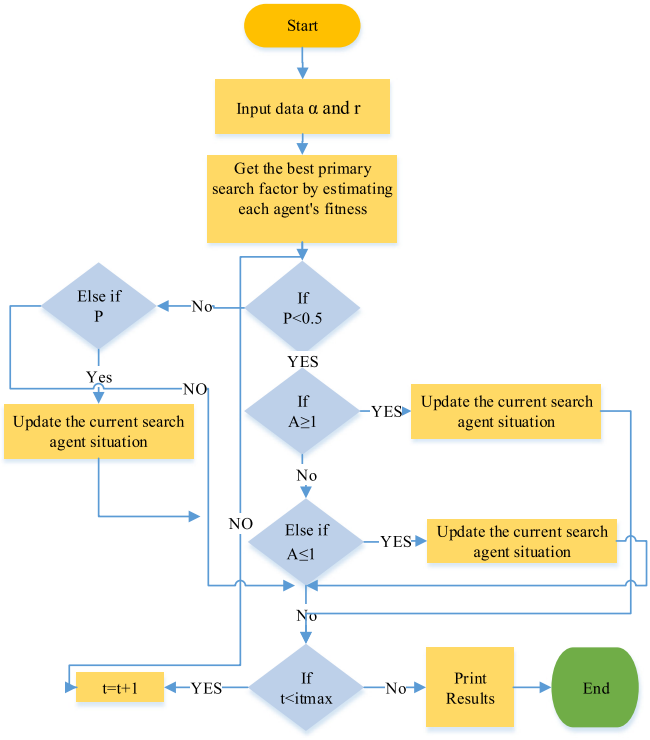

Fig. 6. Whale Optimization Algorithm (WOA).

3. The results

3.1. The hydropower generation

Table 3 indicates the power generation prediction through the hydroelectric power system by RCPs scenarios. The results showed that the power generation from 2021 to 2040 under RCP2.6, RCP4.5, and RCP8.5 decline 10.981 MW, 12.933 MW, 14.765 MW. Also, the power generation from 2041–2060 decline 21.922 MW, 23.649 MW, 26.742 MW. According to the results, in the far future from 2041–2060 the power generation changes

Table 2
The mathematical equations of the test functions to validate the IEFO optimization.

F	Benchmark functions	Equation	F_{min}	Range
F_1	Sphere	$F_1(x) = \sum_{i=1}^{n} x_i^2$	0	[−100,100]
F_2	Schwefe	$F_2(x) = \sum_{i=1}^{n} -x_i \sin(\sqrt{\lvert x_i \rvert})$	−419	[−500,500]
F_3	Ackley	$F_3(x) = -20\exp(-0.2\sqrt{\frac{1}{n}\sum_{i=1}^{n} x_i^2}) - -\exp(\frac{1}{n}\sum_{i=1}^{n}\cos(2\pi x_i)) + 20 + e$	0	[−32,32]
F_4	Matyas function	$F_4(x) = 0.26\left(x_1^2 + x_2^2\right) - 0.48x_1x_2$	0	[10,-10]
F_5	Rastrigin	$F_5(x) = \sum_{i=1}^{d}\left[x_i^2 - 10 \times \cos(2 \times \pi \times x_i) + 10\right]$	0	[-5.12-5.12]
F_6	Bukin 6	$F_6(x) = 100\sqrt{\left(x_2 - 0.01x_1^2\right)} + 0.01\lvert x_1 + 10 \rvert$	0	[−5,15]
F_7	Schwefel2.22	$F_2(x) = \sum_{i=1}^{n} \lvert X_i \rvert + \prod_{i=1}^{n} \lvert x_i \rvert$	0	[−10,10]
	Rosenbrock's	$F_3(x) = \sum_{i=1}^{n-1}[100\left(x_{i+1} - x_i^2\right)^2 + (x_i - 1)^2]$		[−30,30]
	Hybrid Composition Functions	$F_8(x) = (\frac{1}{500} + \sum_{j=1}^{25}\frac{1}{j+\sum_{i=1}^{2}(x_i - a_{ij})^6})^{-1}$		[−65,65]
	Beale function	$f_{(x,y)} = (1.5 - x + xyt)^2 + (2.25 - x + xy^2)^2 + (2.625 - x + xy^3)^2$	0	[−4.5,4.5]
	Booth function	$f(x,y) = (x + 2y - 7)^2 + (2x + y - 5)^2$	0	[−10,10]
	Lévi function N.13	$f(x,y) = sin^2 3\pi x + (x-1)^2(1 + \sin^2 3\pi x) + (y-1)^2(1 + \sin^2 2\pi y)$	0	[−10,10]
	Goldstein--Price function	$f(x,y) = \left[1 + (x + y + 1)^2\left(19 - 14x + 3x^2 - 14y + 6xy + 3y^2\right)\right][30 + (2x - 3y)^2\left(18 - 32x + 12x^2 + 48y + 36xy + 27y^2\right)]$	0	[2,−2]

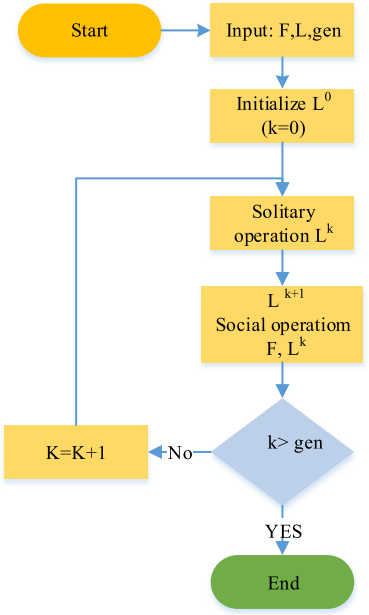

Fig. 7. Locust Search Optimization (LS).

decreases will intensify in the far future. The results show, power generation in the future will be affected by climate change. Electricity production will be declining in the future. The decrease in hydropower production in the future is due to changing rainfall patterns. Changes in precipitation patterns and decreases in precipitation are due to rising temperatures. Reduction of rainfall in the future will reduce the inflow to the reservoir and thus reduce the reservoir level of the hydropower plant. Also, due to the increase in temperature, the evaporation rate of the reservoir will increase, which in turn can reduce the surface of the reservoir. Therefore, generators will face a reduction in input current, and as a result, the electricity generated by the input current will be less than in the past.

Figs. 9 and 10 show the monthly power generation by RCPs. The results showed that the power generation of the hydroelectric system has a non-uniform trend in different months of the year. In some months the upward trend and in some the downward trend. The simulated results of future power generation by RCPs showed that under all three scenarios, power generation in May, Jun, and Jul, has a decreasing trend and in Oct, Nov, and Dec, has an increasing trend. The reason for the decrease in the power production of the month's May, Jun, and Jul is the decrease in rainfall and increase in temperature and evaporation. Also, the reason for the increase in power production in the months Oct, Nov, and Dec, is the increase in seasonal rainfall and the rising level of the reservoir of the hydropower plant. Although in all three scenarios, the trend of monthly changes is similar, the comparison of the projected monthly power generation under the RCPs has been determined, which in RCP 8.5 scenarios less than other scenarios of power generation.

3.2. The energy demand

3.2.1. The selection of the best algorithm to optimal ANN model

Table 4 shows the results of comparing IEFO optimization algorithm with other studied algorithms, based on average (average value of results), STD (standard deviation value), minimum (lower value), and maximum (higher value), respectively, for 20 runs. The value of total algorithms for the population size is 120 and for the iteration, numbers are 180.

Table 4 the results defines that among the literature optimization algorithms, the IEFO optimization algorithm has the less standard division and the most accuracy. Also, it has the most reliability in the different run than the other metaheuristic algorithms. The results define that suggested optimization algorithms have the best performance to forecast energy demand. Because the suggested optimization algorithm with refining optimization problems has less standard division and the most accuracy. Therefore, these metaheuristic algorithms have been used for predicting energy demand.

In this research, 80% of the input data has been utilized to train, 20% of the input data has been used to test. Population, GDP, temperature, precipitation, and evaporation have been trained, tested on the optimized ANN models. Figs. 11 and 12 show

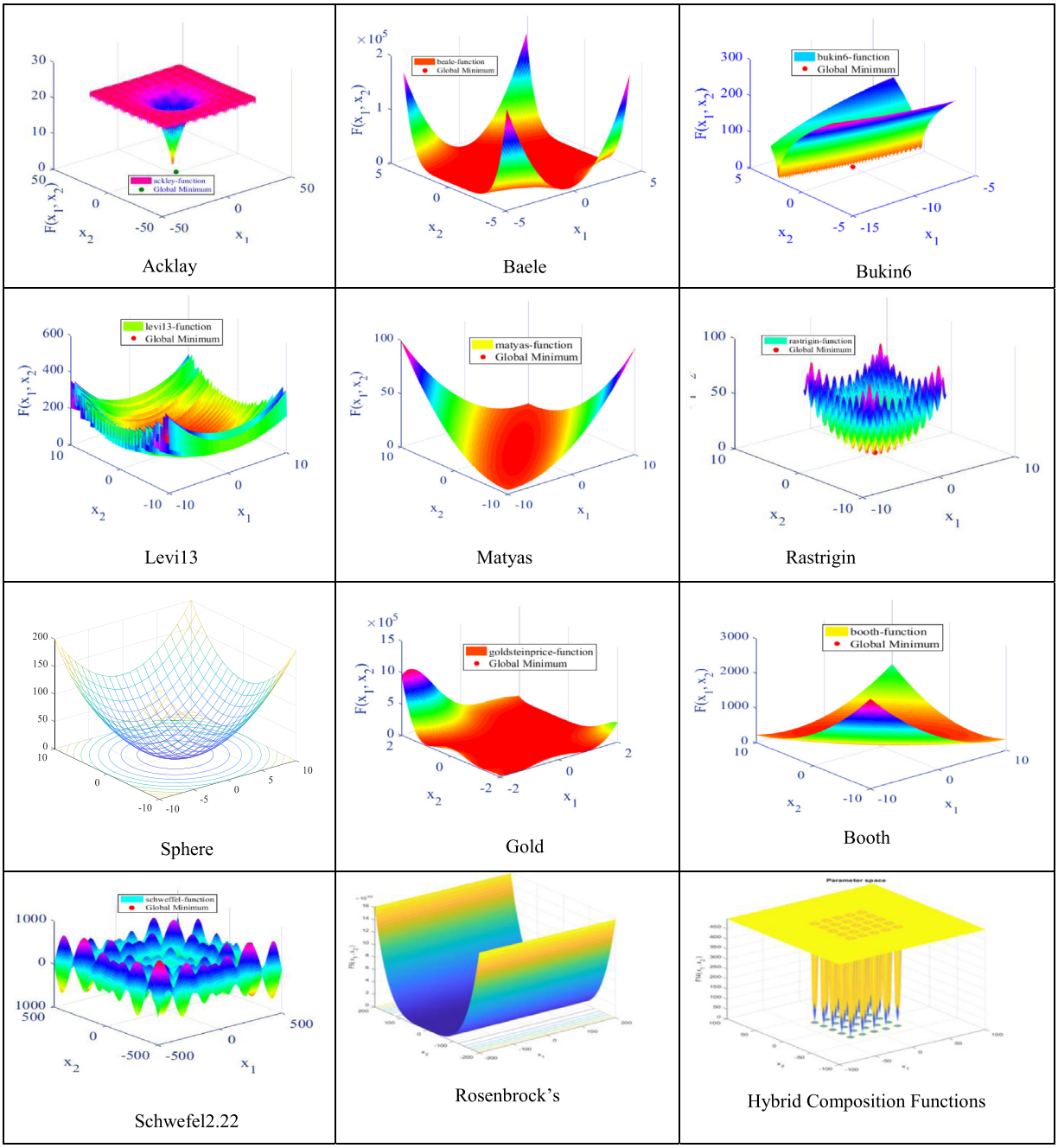

Fig. 8. 2D version of used the benchmark functions.

Table 3
Annual mean hydroelectric power generation.

Hydropower generation	Historical	Near future (2021–2040)			Far future(2041–2060)		
		RCP 2.6	RCP 4.5	RCP8.5	RCP 2.6	RCP 4.5	RCP8.5
	73.107	62.126	60.174	58.342	51.185	49.458	46.365

the correlation coefficients (R^2) and the Root Mean Square Error (RMSE) of the prediction process through the optimized ANN models in training and testing steps.

The results obtained from Figs. 11 and 12 show that among the optimized models, the ANN-IEFO model has the highest correlation and the lowest error value in the simulation of input variables. This model provides the best results in both training and testing steps. Therefore, among the proposed models, the artificial neural network optimized by the IEFO algorithm provides acceptable results for simulating the input variables. Therefore, this model will have a better ability to predict energy demand in the future. Examining Figs. 11 and 12 it is also found that the maximum correlation belongs to the population and then temperature parameters. The population parameters in train and test steps have $R^2 = 0.676$ value and $R^2 = 0.624$ and the

Table 4
The validation results of the IEFO compared with studied algorithms.

Algorithms	LS		ALO		WOA		EFO		IEFO	
Functions	Med	SDT	Med	SDT	Med	SDT	Med	SDT	Med	SDT
Sphere	9.18E−10	9.07E−11	8.73E−10	8.44E−11	8.28E−10	8.59E−11	3.69E−16	4.06E−17	2.46 E-18	2.85E−19
Schwefe	8.96	6.22	2.79	1.31	1.82E−1	2.69E−1	5.16E−9	4.71E−10	6.92E−9	5.68E−10
Ackley	4.88E−9	3.07E−10	5.68E−9	5.01E−10	6.24E−9	6.12E−10	7.19E−10	1.69E−11	8.65 E-10	1.17E−11
Matyas	4.12E−10	3.62E−11	3.74E−11	3.83E−12	4.48E−11	4.14E−12	5.36E−11	5.09E−12	6.15E−11	6.94E−12
Rastrigin	5.78E−8	5.51E−8	2.41E−10	2.81E−11	4.85E−12	4.68E−13	5.57E−12	5.45E−13	4.90 E-14	4.14E−15
Bukin 6	3.45E−11	3.23E−11	3.14E−12	4.76E−12	4.14E−12	4.86E−12	6.88E−12	6.81E−13	7.75E−12	7.87E−13
Schwefel2.22	4. 83E−8	1.58E−8	3.31E−10	2.11E−11	3.15E−12	3.24E−13	4.37E−12	4.83E−13	3.83E−14	2.01E−15
Rosenbrock's	1.14	1.19	1.0 87	1.096	0.95	0.098	0.43	0.031	0.16	0.015
Composition	3.61	0.15	2.71	0.25	1.54	1.38	1. 29	1.12	0.596	0.11
Beale	0. 95	0.83	0.14	0.16	0.12	0. 17	0.058	0.043	0.029	0.027
Booth	3.18E−10	2.84E−11	2.73E−10	2.64E−11	2.56E−10	2.36E−11	1.36E−10	1.09E−11	1.15E−10	1.04E−11
Lévi N.13	13.80	11.53	10.73	10.47	7.80	7.50	3.83	1.42	0.08	0.05

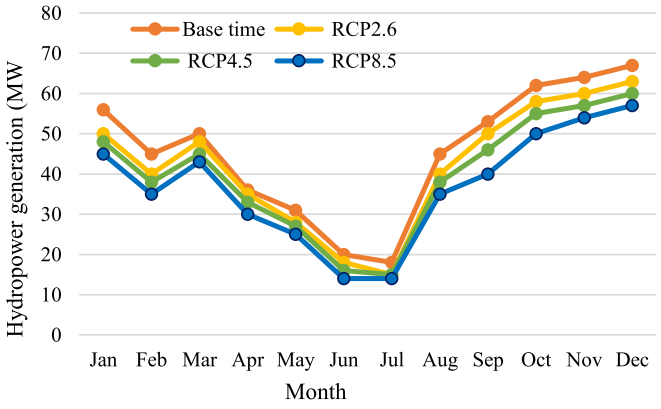

Fig. 9. Monthly electricity generation by RCPs for the near future.

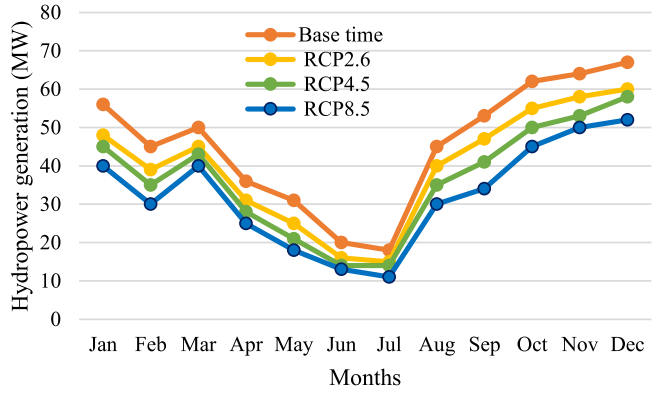

Fig. 10. Monthly electricity generation by RCPs for far future.

temperature in train and test steps have $R^2 = 0.544$ value and $R^2 = 0.583$. The results of the correlation parameters show that changes in population and temperature can have the most impact on energy demand.

According to the effect of these two parameters in forecasting energy demand the sensitivity analysis of population uncertainty and temperature variables has been examined. Fig. 13 shows the sensitivity analysis of population and temperature uncertainty for training and testing steps. Table 5 also displays the correlation and error sensitivity analysis of these variables in the training and testing stages.

Table 6 shows the contribution of optimized artificial neural network parameters in energy demand forecasting. According to the results, it is known that the population has the most contribution and impact on energy demand, followed by temperature, GDP, rainfall, inflation, and finally evaporation of the reservoir surface of the hydropower plant. Increasing population growth is one of the influential factors in increasing energy demand. Increasing population increases energy consumption in society. So the energy demand will increase. Also, due to the increase in temperature, the use of cooling devices in the community increases, which in turn requires energy. Along with the increase of population and temperature, with the development of the welfare industry, people in the society also increase. Therefore, the use of cooling tools will be more.

3.2.2. The energy demand prediction

Fig. 14 shows the energy demand forecasting for the near future and far future through The ANN-IEFO model. The results showed that the annual electricity demand has increased from 2021 to 2040 by about 513 MW compared to the base period. Also, the energy demand has increased from 2041–2060 by about 1168 MW. The intensity of electricity demand in the far future is most than in the near future. The reason is the increase in population and the development of industry and the increase in GDP and temperature.

Also, Fig. 15 shows the changes in energy demand in different months for the near and far next 20 years.

The results of Fig. 15 show that in the coming years, the temperature will increase compared to the current period. Therefore, we will face hotter and drier summers and the use of cooling devices in hot seasons will be more than the current time. According to the results, it is known, the most of the temperature fluctuations and energy demand belong to different seasons of the year. Seasonal variation causes sharp fluctuations in energy demand. In hot seasons, energy demand increases due to rising temperatures, because the use of cooling devices increases. According to the results of the monthly prediction, it is found, the energy demand in the warm season, its changes are more than in the cold season. The results define, for near compared to the current time in May, Jun, and Jul about 266 MW 235 MW, and 368 MW and in far future 310MW, 360 MW, and 475 MW has been increased. The sharp increase in energy demand in hot seasons in the far future is more than near future because the temperature will rise more sharply and due to low rainfall, the society will face drought.

3.3. Fluctuations between hydroelectric power generation and energy demand

The results of the previous sections define that the energy demand under climatic conditions in different seasons, especially in summer, has more severe fluctuations, while hydroelectric power generation has a slow upward trend. So that in summer, when the energy demand is high, according to the weather conditions, the production of hydropower is at its minimum.

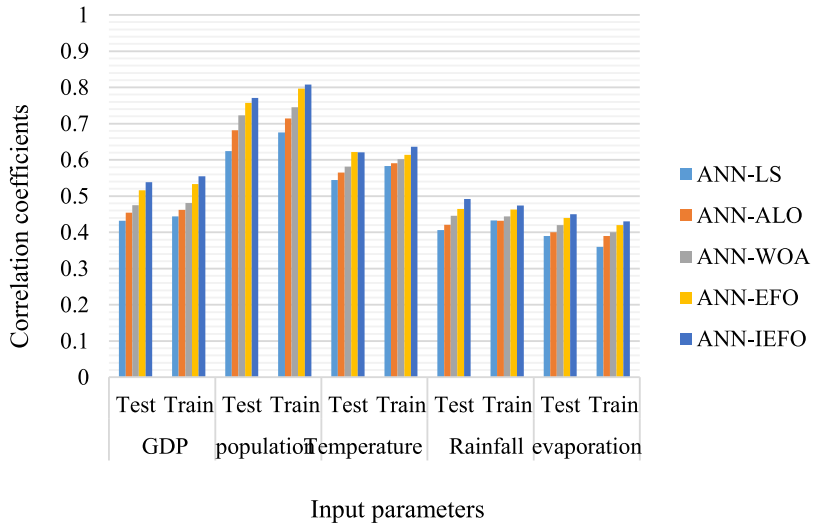

Fig. 11. Correlation of optimized ANN models.

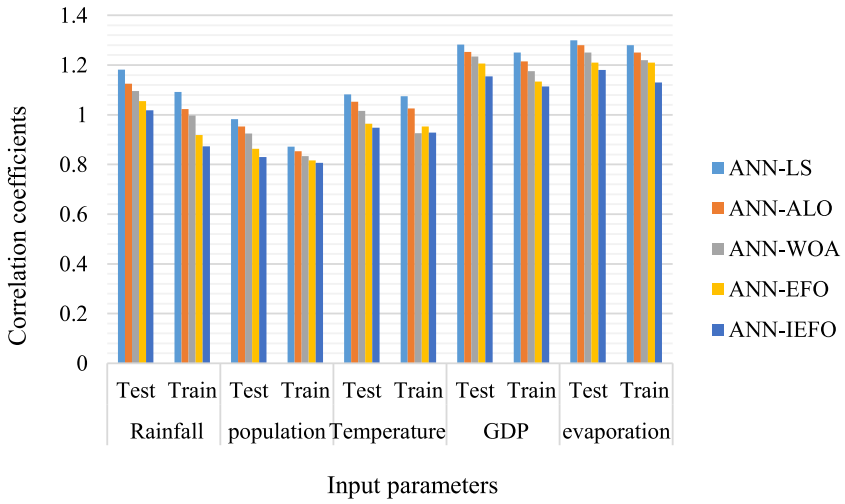

Fig. 12. Error value of optimized ANN models.

Table 5
The correlation and error of uncertainty analysis of forecasting population and GDP variables.

Statistical index	Population				Temperature			
	Train step		Test step		Train step		Test step	
	Lower bound	Upper bound	Lower bound	Upper bound	Lower bound	Upper bound	Lower bound	Upper bound
R^2	0.88	0.78	0.79	0.67	0.77	0.74	0.72	0.67
RMSE	0. 71	0.73	0.81	0.83	0.72	0.74	0.86	0.91

Table 6
The contribution of input variables of predicting energy demand.

Input parameters	Population	GDF	Temperature	Precipitation	Inflation	Evaporation
Contribution (%)	25	21	23	17	10	4

Therefore, the increase in energy demand, especially in summer, makes it possible to use other resources in the region for energy supply. In this section, we have examined the proportion of total energy generation to hydropower production to predict fluctuations in hydropower production and electricity demand in the future. Table 7 illustrates the proportion between the hydroelectric power system and energy demand. According to the forecasting of hydropower generation by RCPs scenarios, it is known that hydropower energy generation is declined in the near future and far future. Therefore, the proportion of total energy generation to hydroelectric power generation will decline. The results of forecasting by RCP8.5 show that the proportion of total energy generation to hydroelectric power generation is lowest compared to other RCPs. Also, the results define that this proportion in the far future is more significant compared to the

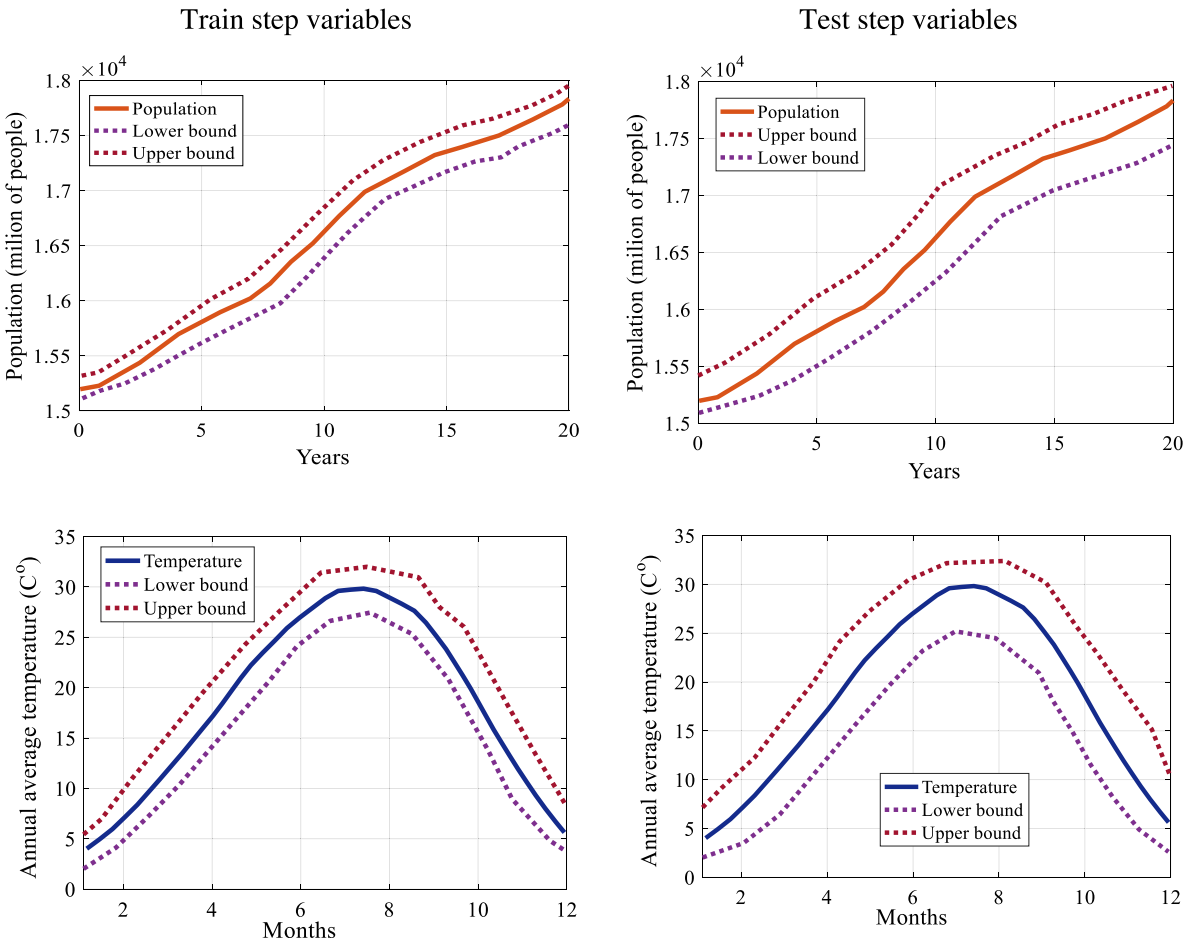

Fig. 13.

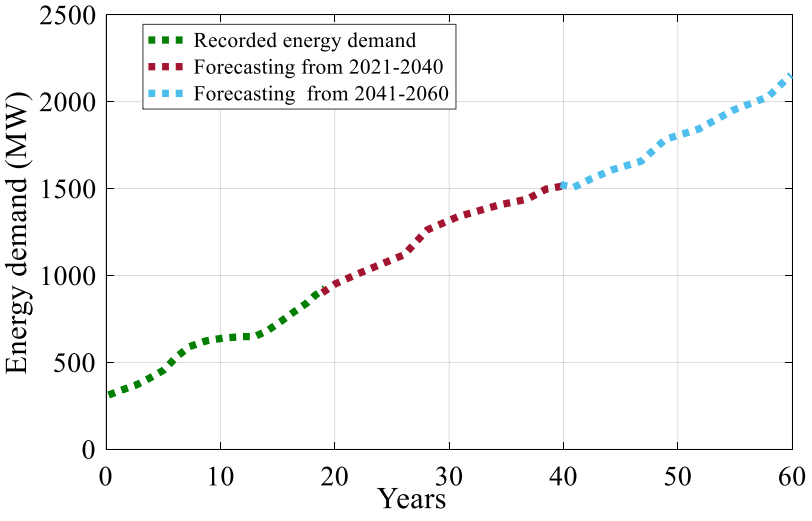

Fig. 14. The forecasted annual energy demand through the ANN-IEFO model.

near future. Because in far future we will face severe climate change.

After determining the proportion between energy produced by the hydropower plant and the total energy produced fluctuations between hydropower production and energy demand is examined. Table 8 shows the monthly fluctuations in hydropower generation and electricity demand in different months for each near and distant future.

The results of the table above showed that the amount of fluctuations in energy demand in the months Mar, Jun, and Jul is more severe than other months of the year. Based on the results, it has been determined that the production of hydropower in these months is at its lowest level, while the highest electricity demand belongs to these months. In Oct, Nov, and Dec the amount of electricity production has an increasing trend due to seasonal rains and the filling of the reservoir, but the demand for

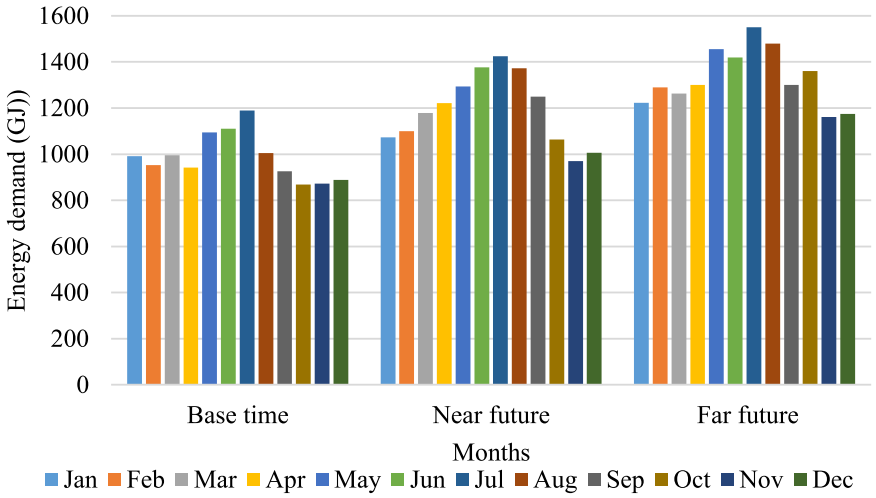

Fig. 15. The prediction monthly energy demand.

Table 7
The proportion of hydroelectric power generation to total energy generation.

The proportion of hydroelectric power generation to total energy generation (%)	Observed	Near future (2021–2040)			Far future (2041–2060)		
		RCP 2.6	RCP 4.5	RCP8.5	RCP 2.6	RCP 4.5	RCP8.5
	21.64	20.21	18.11	15. 64	12.37	10.78	9.16

Table 8
The monthly fluctuations of hydroelectric power generation and energy demand.

The fluctuations of the monthly (%)				
Months	Near future (2021–2040)		Far future (2041–2060)	
	Energy demand	Hydropower generation	Energy demand	Hydropower generation
Jan	0.38	0.78	0.45	0.68
Feb	0.42	0.77	0.46	0.61
Mar	0.43	0.67	0.53	0.57
Apr	0.49	0.55	0.56	0.55
May	0.51	0.53	0.58	0.4
Jun	0.55	0.51	0.61	0.39
Jul	0.81	0.23	0.71	0.18
Aug	0.86	0.21	0.76	0.12
Sep	0.83	0.22	0.45	0.15
Oct	0.41	0.5	0.46	0.41
Nov	0.49	0.51	0.53	0.43
Dec	0.51	0.53	0.56	0.45

energy in this month has a slowly increasing trend. The results show that there is an imbalance between the power generation of the hydropower system and the electricity demand. Also, fluctuations in energy demand are more severe than fluctuations in the power generation of the hydraulic system. Therefore, due to these fluctuations, energy supply for different uses may face problems. These changes in the distant future from 2041 to 2060 will be more severe than the first 20 years.

3.4. Investigate the Gap of demand-supply of energy under the influence of climate changes

Table 9 shows the fluctuations of energy demand and energy supply in arid, normal, and humid weather conditions.

The energy supply and energy demand gap are sharper in dry conditions than in other climatic conditions. These changes will be most in the far future (second 20 years). The results show that in normal and humid conditions, however, hydropower generation will increase due to seasonal rainfall, and the gap between demand and energy supply will decrease. But these changes will be more than the base period and the probability of not providing energy in the future will be higher than now. Therefore, in the future, we will face an increase in the gap between the energy demand and energy supply in all periods, but in dry conditions, these changes are more significant. Therefore, in the future, other energy sources should be used to compensate for the gap between demand and energy supply. This requires the installation of other electrical sources to meet the demand for higher capacity electricity in dry years.

3.5. The climate change impact on GHG concentration

According to the results from forecasting the impact of climate change on hydropower generation and energy demand, examining the fluctuations of hydropower generation and energy demand and, the gap between demand and energy supply in different climatic conditions has been observed that t between hydroelectric power generation and energy demand is not balanced. Hydropower generation cannot meet energy demand in the coming years. Therefore, energy demand should be provided through other energy resources. The other resource such as fossil fuels will raise greenhouse gas concentration. The energy resources in the region, except for the hydropower plant, include the Manjil wind turbine farm, photovoltaic systems, coal mines, or a mixture of these energy sources. Table 10 illustrates the average yearly greenhouse gas emissions in the near and far future under climatic scenarios.

According to Table 10, the most GHG emissions belong to the RCP8.5 forecast and the minimum GHG emissions belong to the RCP2.6 forecast. The less GHG emission through RCP2.6 in the near future has been forecasted about 14.03%, 10.09%, 28.21%, and 17.96% for the wind turbine field, photovoltaic system, coal mines, and mixed energy sources and in the far future assessed approximately 7.14%, 4.76%, 12.33%, and 9.7%, respectively. The

Table 9
The Gap between demand-supply in different conditions.

Period	Historical			Near future (2021–2040)			Far future (2041–2060)		
Climate condition	Dry	Normal	Wet	Dry	Normal	Wet	Dry	Normal	Wet
Demand	436	482	336	511	488	346	553	493	350
Supply	387	457	292	449	458	308.5	425.2	371.6	320.8

Table 10
The climate change impact on GHG concentration.

GHG emission (MMTCO2/yr)							
Energy resources	Historical	Near future (2021–2040)			Far future (2041–2060)		
		RCP 2.6	RCP 4.5	RCP8.5	RCP 2.6	RCP 4.5	RCP8.5
Coal mines	312	356	364	441	402	423	556
Wind turbine	26	28	29	32	30	32	35
Photovoltaic system	20	21	21	23	22	23.5	24.5
The mixture of energy	93	103	106	121	112	126	135

most GHG emissions under the RCP8.5 scenario have been forecasted 18.21%, 15.31%, 38.08%, and 28.40% for the wind turbine field, photovoltaic system, coal mines, and mixed energy sources in the near future. Also, the most GHG emissions under the RCP8.5 scenario in the far future have been forecasted 20.35%, 16.24%, 39.55%, and 30.01%, respectively. The results achieved determine that although increasing power generation by other energy resources will supply energy demand in the future, increase GHG concentration. Therefore, to energy meet, clean energy should be used such as wind turbines and photovoltaic more compared to fossil fuel. Therefore, in addition to the reduced gap between energy demand-supply, GHG concentration is also decreased.

4. Conclusion

In this research, the effects of climate change on hydroelectric power generation, energy demand, the balance between energy supply–demand and greenhouse gas concentration were studied. The RCPs were utilized to predict power generation. In this study, an artificial neural network (ANN) optimized by Improved Electromagnetic Field Optimization (IEFO) algorithms was used to predict energy demand. Finally, fluctuations in hydropower generation and energy demand in different seasons of the year and the gap between demand and energy supply in different climatic conditions were analyzed. The results show that with increasing temperature and changing rainfall patterns, hydropower generation for the near future under RCP2.6, RCP4.5, and RCP8.5 will decrease by about 10.981 MW, 12.933MW, 14.765MW, and for the distant future by will be reduced about decline 21.922 MW, 23.649 MW, and 26.742 MW. The energy demand prediction through the ANN-IEFO model for the near and far future will rise compared to the current time about 513 MW and 1168 MW, respectively. The results also showed that due to the increase in the gap between demand and energy supply, the likelihood of using other sources of fossil fuels and coal mines will increase. Therefore, the concentration of greenhouse gases will increase.

CRediT authorship contribution statement

Li-Na Guo: Conceptualization, Data curation, Writing – original draft, Writing – review & editing. **Chen She:** Conceptualization, Data curation, Writing – original draft, Writing – review & editing. **De-Bin Kong:** Conceptualization, Data curation, Writing – original draft, Writing – review & editing. **Shuai-Ling Yan:** Conceptualization, Data curation, Writing – original draft, Writing – review & editing. **Yi-Peng Xu:** Conceptualization, Data curation, Writing – original draft, Writing – review & editing. **Majid Khayatnezhad:** Conceptualization, Data curation, Writing – original draft, Writing – review & editing. **Fatemeh Gholinia:** Conceptualization, Data curation, Writing – original draft, Writing – review & editing.

Declaration of competing interest

The authors declare that they have no known competing financial interests or personal relationships that could have appeared to influence the work reported in this paper.

Acknowledgment

This work was supported by the Project of Hebei Province for Department of Education Youth Fund, China (Grant No. QN2020520), and Hebei Province for Science and Technology Department Science Popularization, China (Grant No. 20550301K).

References

Abedinpourshotorban, H., et al., 2016. Electromagnetic field optimization: a physics-inspired metaheuristic optimization algorithm. Swarm Evol. Comput. 26, 8–22.
Antonopoulos, I., et al., 2020. Artificial intelligence and machine learning approaches to energy demand-side response: A systematic review. Renew. Sustain. Energy Rev. 130, 109899.
Bhatta, B., et al., 2019. Evaluation and application of a SWAT model to assess the climate change impact on the hydrology of the Himalayan River Basin. Catena 181, 104082.
Bouchekara, H., 2020. Solution of the optimal power flow problem considering security constraints using an improved chaotic electromagnetic field optimization algorithm. Neural Comput. Appl. 32 (7), 2683–2703.
Bouchekara, H., Zellagui, M., Abido, M.A., 2017. Optimal coordination of directional overcurrent relays using a modified electromagnetic field optimization algorithm. Appl. Soft Comput. 54, 267–283.
Cai, W., et al., 2019. Optimal bidding and offering strategies of compressed air energy storage: A hybrid robust-stochastic approach. Renew. Energy 143, 1–8.
Chen, S., 2009. Locust swarms-a new multi-optima search technique. In: 2009 IEEE Congress on Evolutionary Computation. IEEE.
Chen, W., Wei, P., Peng, Y., Impacts of climate change on monthly electricity consumption: A case of Tianjin, China. Polish J. Environ. Stud..
Chen, Y.H., et al., 2016. Electric load forecasting based on a least squares support vector machine with fuzzy time series and global harmony search algorithm. Energies 9 (2), 70.
Cuevas, E., Cortés, M.A.D., Navarro, D.A.O., 2016. Optimization based on the behavior of locust swarms. In: Advances of Evolutionary Computation. Methods and Operators, Springer, pp. 101–120.
Dehghani, M., et al., 2019. Prediction of hydropower generation using grey wolf optimization adaptive neuro-fuzzy inference system. Energies 12 (2), 289.
Di Piazza, A., et al., 2021. An artificial neural network-based forecasting model of energy-related time series for electrical grid management. Math. Comput. Simulation 184, 294–305.
Dinaharan, I., et al., 2020. Application of artificial neural network in predicting the wear rate of copper surface composites produced using friction stir processing. Australian J. Mech. Engi. 1–12.

Emodi, N.V., Chaiechi, T., Alam Beg, A.R., 2018. The impact of climate change on electricity demand in Australia. Energy Environ 29 (7), 1263–1297.
Faiz, M.A., et al., 2018. Performance evaluation of hydrological models using ensemble of general circulation models in the northeastern China. J. Hydrol. 565, 599–613.
Fan, G.-F., et al., 2013. Support vector regression model based on empirical mode decomposition and auto regression for electric load forecasting. Energies 6 (4), 1887–1901.
Fan, X., et al., 2020. High voltage gain DC/DC converter using coupled inductor and VM techniques. IEEE Access 8, 131975-131987.
Fatemi, et al., 2019. Collocation method for differential variational inequality problems. Int. J. Numer. Modelling, Electron. Netw. Devices Fields 32 (1), e2466.
Feng, Y., et al., 2018. Long-term hydropower generation of cascade reservoirs under future climate changes in Jinsha river in southwest China. Water 10 (2), 235.
Fonseca, A., Santos, J., 2019. Predicting hydrologic flows under climate change: The Tâmega Basin as an analog for the mediterranean region. Sci. Total Environ. 668, 1013–1024.
Franco, G., Sanstad, A.H., 2008. Climate change and electricity demand in California. Clim. Change 87 (1), 139–151.
Garrido-Perez, J.M., et al., 2021. Impact of climate change on spanish electricity demand. Clim. Change 165 (3), 1–18.
GEDC, 1947. Gilan Electricity Distribution Company. Available from: www.gilanpdc.ir.
Ghiasi, M., Ghadimi, N., Ahmadinia, E., 2019. An analytical methodology for reliability assessment and failure analysis in distributed power system. SN Appl. Sci 1 (1), 44.
Guo, Z., et al., 2021. Novel computer-aided lung cancer detection based on convolutional neural network-based and feature-based classifiers using metaheuristics. Int. J. Imaging Syst. Technol..
Hosseini, H., et al., 2012. A novel method using imperialist competitive algorithm (ICA) for controlling pitch angle in hybrid wind and PV array energy production system. Int. J. Tech. Phys. Prob. Eng (IJTPE) 11, 145–152.
Hu, A., Navid, R., 2020. Brain tumor diagnosis based on metaheuristics and deep learning. Int. J. Imaging Syst. Technol..
Huangpeng, Q., Huang, W., Gholinia, F., 2021. Forecast of the hydropower generation under influence of climate change based on RCPs and developed crow search optimization algorithm. Energy Rep. 7, 385–397.
Inflation, Consumer prices (annual %).
Ingle, K.K., Jatoth, R.K., 2019. An efficient JAYA algorithm with Lé for Non-linear Channel Equalization. Expert Syst. Appl. 112970.
Jakimavičius, D., et al., 2020. Climate change impact on hydropower resources in gauged and ungauged Lithuanian river Catchments. Water 12 (11), 3265.
Kassem, A.A., et al., 2019. Predicting of daily khazir basin flow using SWAT and hybrid SWAT-ANN models. Ain Shams Eng. J..
Khalil, A.J., et al., 2019. Energy efficiency prediction using artificial neural network. Int. Jo. Acad. Pedagogical Res. (IJAPR) 3 (9).
Kim, S., et al., 2019. Development of a consecutive occupancy estimation framework for improving the energy demand prediction performance of building energy modeling tools. Energies 12 (3), 433.
Kitessa, B.D., et al., 2021. Long-term water-energy demand prediction using a regression model: a case study of Addis Ababa city. J. Water Climate Change.
Lal, M., Mishra, S., Kumar, M., 2019. Reverification of antecedent moisture condition dependent runoff curve number formulae using experimental data of Indian watersheds. Catena 173, 48–58.
Le, B., Le, D.P., Tran, M.-T., 2021. Hiding sensitive association rules using the optimal electromagnetic optimization method and a dynamic bit vector data structure. Expert Syst. Appl. 176, 114879.
Leaf-nosed bat, 2009. EncyclopæDia Britannica. Encyclopædia Britannica Online.
Lee, J.-Y., et al., 2019. Feasible ranges of runoff curve numbers for Korean watersheds based on the interior point optimization algorithm. KSCE J. Civil Eng 1–9.
Li, X., Niu, P., Liu, J., 2018. Combustion optimization of a boiler based on the chaos and Levy flight vortex search algorithm. Appl. Math. Model. 58, 3–18.
Li, M.-W., et al., 2021. Chaos cloud quantum bat hybrid optimization algorithm. Nonlinear Dynam. 103 (1), 1167–1193.
Liu, Y., Wang, W., Ghadimi, N., 2017. Electricity load forecasting by an improved forecast engine for building level consumers. Energy 139, 18–30.
Liu, J., et al., 2020. An IGDT-based risk-involved optimal bidding strategy for hydrogen storage-based intelligent parking lot of electric vehicles. J. Energy Storage 27, 101057.
Martínez-Solanas, È., et al., 2021. Projections of temperature-attributable mortality in europe: a time series analysis of 147 contiguous regions in 16 countries. The Lancet Planetary Health 5 (7), e446–e454.
Mason, K., Duggan, J., Howley, E., 2018. Wind generation and carbon dioxide emissions in Ireland using evolutionary neural networks. Energy 155, 705–720.
McGookin, C., Gallachóir, B.Ó., Byrne, E., 2021. An innovative approach for estimating energy demand and supply to inform local energy transitions. Energy 229, 120731.
Meng, Q., et al., 2020. A single-phase transformer-less grid-tied inverter based on switched capacitor for PV application. J. Control, Autom. Electr. Syst 31 (1), 257–270.
Mir, M., et al., 2020. Application of hybrid forecast engine based intelligent algorithm and feature selection for wind signal prediction. Evol. Syst. 11 (4), 559–573.
Mirjalili, S., Lewis, A., 2016. The whale optimization algorithm. Adv. Eng. Softw. 95, 51–67.
Navid, R., et al., 2021. A new design for robust control of power system stabilizer based on moth search algorithm. In: Metaheuristics and Optimization in Computer and Electrical Engineering. Springer, pp. 187–202.
Neto, S.L.R., et al., 2019. Efficacy of Rainfall-Runoff models in loose coupling spacial decision support systems modelbase. Water Resour. Manag 33 (3), 889–904.
OECD, 1948. Organization for Economic Cooperation and Development.
Oo, H.T., Zin, W.W., Kyi, C.T., 2020. Analysis of streamflow response to changing climate conditions using SWAT model. Civil Eng J. 6 (2), 194–209.
Ramezani, Mehdi, et al., 2021. A new improved model of marine predator algorithm for optimization problems. Arab. J. Sci. Eng..
Razmjooy, N., Estrela, V.V., 2019. Applications of Image Processing and Soft Computing Systems in Agriculture.
Razmjooy, N., Madadi, A., Ramezani, M., 2016. Robust control of power system stabilizer using world cup optimization algorithm. Int. J. Inform., Security, Syst. Manag 5 (1), 524–531.
Ren, X., et al., 2021. Predicting optimal hydropower generation with help optimal management of water resources by developed wildebeest herd optimization (DWHO). Energy Rep. 7, 968–980.
Rim, C., et al., 2018. A niching chaos optimization algorithm for multimodal optimization. Soft Comput. 22 (2), 621–633.
Roy, K., Mandal, K.K., Mandal, A.C., 2019. Ant-Lion optimizer algorithm and recurrent neural network for energy management of micro grid connected system. Energy 167, 402–416.
SCI, 1965. Statistical Center of Iran.
Song, S., Jia, H., Ma, J., 2019. A chaotic electromagnetic field optimization algorithm based on fuzzy entropy for multilevel thresholding color image segmentation. Entropy 21 (4), 398.
Tan, Y., et al., 2021. The impact of extreme climate change on the fluctuation of electricity energy demand——Evidence from China's prefecture-level cities. In: E3S Web of Conferences.
Toste, R., de Freitas Assad, L.P., Landau, L., 2018. Downscaling of the global HadGEM2-ES results to model the future and present-day ocean conditions of the southeastern Brazilian continental shelf. Clim. Dynam. 51 (1), 143–159.
Unutmaz, Y.E., et al., 2021. Electrical energy demand forecasting using artificial neural network. In: 2021 3rd International Congress on Human-Computer Interaction, Optimization and Robotic Applications (HORA). IEEE.
Wang, H., Wu, X., Gholinia, F., Forecasting hydropower generation by GFDL-CM3 climate model and hybrid hydrological-Elman neural network model based on Improved Sparrow Search Algorithm (ISSA). In: Concurrency and Computation: Practice and Experience, p. e6476.
Xu, Z., et al., 2020. Computer-aided diagnosis of skin cancer based on soft computing techniques. Open Medicine 15 (1), 860–871.
Ye, H., et al., 2020. High step-up interleaved dc/dc converter with high efficiency. Energy Sour, A: Recovery, Utilization, and Environmental Effects 1–20.
Yu, D., Ghadimi, N., 2019. Reliability constraint stochastic UC by considering the correlation of random variables with Copula theory. IET Renew. Power Gener. 13 (14), 2587–2593.
Yu, D., et al., 2019. System identification of PEM fuel cells using an improved elman neural network and a new hybrid optimization algorithm. Energy Rep. 5, 1365–1374.
Yu, D., et al., 2020. Energy management of wind-PV-storage-grid based large electricity consumer using robust optimization technique. J. Energy Storage 27, 101054.
Yuan, Z., et al., 2020. Probabilistic decomposition-based security constrained transmission expansion planning incorporating distributed series reactor. IET Gener., Trans. Distrib 14 (17), 3478–3487.